Charge states of a hydrogen defect with a local vibrational mode at 3326 cm^{-1} in ZnO

F. Herklotz,* E. V. Lavrov, Vl. Kolkovsky, and J. Weber
Technische Universität Dresden, 01062 Dresden, Germany

M. Stavola
Lehigh University, Bethlehem, Pennsylvania 18015, USA
(Received 31 May 2010; published 13 September 2010)

An IR absorption study is presented of a hydrogen defect in ZnO that gives rise to a local vibrational mode at 3326 cm^{-1} [M. D. McCluskey *et al.*, Appl. Phys. Lett. **81**, 3807 (2002)]. It is shown that a subband gap illumination results in the appearance of a new IR absorption line at 3358 cm^{-1} at the expense of the main signal at 3326 cm^{-1}. Based on the anticorrelation between the two lines as well as on the results of isotope substitution experiments it is concluded that both signals are due to stretch modes of an O-H bond of the same defect in different charge states. The energy of the subband gap light strongly suggest that this defect has a deep rather than shallow level in the band gap of ZnO. Additionally, the results on thermal stability, uniaxial stress response, and temperature dependence of the transition rates between the two charge states of this defect are presented.

DOI: 10.1103/PhysRevB.82.115206 PACS number(s): 61.72.−y, 78.30.Fs, 71.55.Gs

I. INTRODUCTION

Hydrogen is a common impurity in ZnO that can be unintentionally introduced into material at different stages of semiconductor processing. From the technological point of view, interest in hydrogen comes from its strong influence on electrical properties of ZnO which occurs, for example, via formation of shallow donor states and/or acceptor passivation.[1–11]

Isolated hydrogen in ZnO is located at the bond-centered lattice site oriented along the *c* axis, H_{BC}.[12] Hydrogen forms a strong covalent bond with the neighboring oxygen atom, which gives rise to a local vibrational mode (LVM) at 3611 cm^{-1} measured at 10 K.[13] H_{BC} is a shallow donor with an ionization energy of 53 meV.[12] Excitons bound to this defect result in a luminescence line at around 3360.1 meV.[12] Bond-centered hydrogen is unstable at temperatures above 110 °C.[12] Its stability is governed by the diffusion process with the subsequent trapping by other defects and/or formation of interstitial hydrogen molecule H_2.[14]

Another hydrogen-related shallow donor in ZnO is hydrogen bound to the oxygen vacancy, H_O.[4,12] The ionization energy of H_O is 47 meV. The recombination of excitons bound to H_O gives rise to the I_4 photoluminescence line at 3326.8 meV.[12] This defect anneals out at temperatures above 500 °C and is a dominant shallow donor in some ZnO crystals grown by chemical vapor transport.[8,15]

In addition to the hydrogen shallow donors, the detailed spectroscopic features of many acceptor-hydrogen complexes were studied and contributed to our understanding of the microscopic structure of these complexes.[16–21] Despite the considerable progress achieved in the last decade, a number of hydrogen-related issues remains controversial. The subject of our present study is a defect observed by McCluskey *et al.*[9] We label it XH (XD in case of deuterium).

XH gives rise to an absorption line at 3326 cm^{-1} due to the LVM of the O-H bond which forms an angle of about 110° with the *c* axis. Interestingly, the intensity of the 3326 cm^{-1} IR line depends on the starting material: the absorption signal was shown to be stronger in melt-grown ZnO provided by Cermet Inc.[9,22,23] than in samples grown via chemical vapor transport obtained from Eagle-Picher[24] or vapor phase grown ZnO.[13,24]

The microscopic structure of XH remains controversial. Initially, the defect was tentatively assigned to isolated hydrogen located at an antibonding lattice site aligned perpendicular to the *c* axis.[23] More recently, a calcium-hydrogen (CaH) complex[25,26] and a Zn vacancy passivated by a hydrogen atom in the negative-charge state, $V_{Zn}H^-$, were proposed as alternative models.[27]

It was also established that illumination of ZnO samples with subband gap light results in a decrease in the intensity of the 3326 cm^{-1} line.[24,28] This behavior was tentatively interpreted as a transition of the XH defect to another charge state. No IR absorption line, however, was observed which could be assigned to the LVM of XH in the other charge state.

In this paper, we present an IR absorption study of the XH defect under subband gap illumination. It is shown that such illumination results in the appearance of an IR absorption line at 3358 cm^{-1} at the expense of the main signal at 3326 cm^{-1}. Isotope substitution experiments, transition rates at different temperatures, uniaxial stress data, and thermal stability of the XH defect are reported. In view of these experimental findings the microscopic structure of the XH defect is discussed.

II. EXPERIMENTAL PROCEDURE

The ZnO samples used in this work were commercial melt-grown ZnO *c*-cut $5.2\times5.2\times0.5$ mm^3 wafers with a resistivity of 50–200 Ω cm purchased from Cermet, Inc.

Hydrogen and/or deuterium were/was introduced into the samples via thermal treatments in sealed quartz ampoules filled with hydrogen and/or deuterium gas (pressure of 0.5 bar at room temperature). The treatments were performed at a temperature of 725 °C for one hour and were terminated by quenching to room temperature in water.

In order to study the thermal stability of the hydrogen defects discussed in this paper, the spectra were recorded after each step in a series of isochronal heat treatments (anneals) at temperatures in the range from 50 to 480 °C. Each anneal had a duration of 30 min and was carried out in an argon atmosphere.

For uniaxial stress measurements two samples were cut with the dimensions of $5.1\times2.3\times0.5$ mm^3 and $5.2\times2.5\times0.5$ mm^3 with the longest side parallel either to $[10\bar{1}0]$ or $[1\bar{2}10]$, respectively.

Infrared absorption spectra were recorded with a BOMEM DA3.01 Fourier transform spectrometer equipped with a globar or quartz light source, a CaF_2 beamsplitter and a liquid-nitrogen-cooled InSb detector. The spectral resolution was 0.05–1 cm^{-1}.

Subband gap illumination of the ZnO samples was normally performed with the 0.633 μm line (1.96 eV) of a HeNe laser with a power of approximately 3 mW at a temperature of 7 K. To investigate the wavelength dependence of photoinduced effects the quartz lamp of the Fourier spectrometer was employed. In this case different low-pass filters were placed between the light source and the entrance window of the optical cryostat.

Uniaxial stress measurements were carried out with a home-built stress rig mounted in the gas-flow cryostat equipped with ZnSe windows. The stress was supplied by a pneumatic cylinder and transferred via a push rod to the longest side of the sample.

IR absorption measurements were performed at 7 K unless noted otherwise. Polarized light was produced by a wire-grid polarizer with a KRS-5 substrate. More details about Fourier transform infrared (FTIR) setup and the uniaxial stress rig can be found elsewhere.[29]

III. RESULTS

A. General properties of the IR lines

IR absorption spectra of a melt-grown ZnO sample treated with H_2 gas are presented in the right panel of Fig. 1. Spectrum (a) was taken without subband gap illumination whereas spectra (b) and (c) were measured after illumination with the HeNe laser for 15 min and 60 min, respectively. Only the 3326 cm^{-1} line of the XH$^{(n)}$ complex is seen in the spectrum without illumination.[9] Here, we employ the n superscript to denote the charge state (yet unknown) of the defect.

The subband gap light results in the decrease in the 3326 cm^{-1} line intensity, as can be seen from the spectra (b) and (c) in the figure. What is important, the illumination also results in the appearance of a weak IR absorption line at 3358 cm^{-1}.

We note that the effect of the subband gap light on the intensity of the 3326 cm^{-1} line was also studied by Shi *et al.*[24] and Nickel.[28] No extra line, however, was reported by these authors, which would appear at the expense of the main signal at 3326 cm^{-1}. The weakness of this line could presumably explain why the photoinduced signal has escaped observation so far.

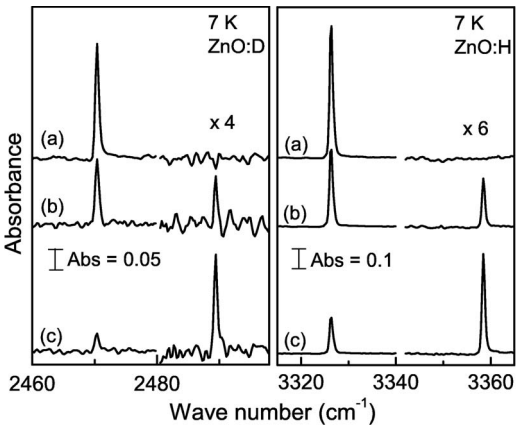

FIG. 1. IR absorption spectra obtained from ZnO samples after thermal treatment in the H_2 (right panel) and D_2 gas (left panel) at 725 °C. The spectra were recorded without (a) and under subband gap illumination with a HeNe laser for (b) 15 min and (c) 60 min.

To get insight into the nature of the 3358 cm^{-1} line, IR absorption spectra for a melt-grown ZnO sample treated with D_2 gas were also recorded. They are presented in the left panel of Fig. 1. Without the subband gap illumination only the line due to the XD$^{(n)}$ complex at 2471 cm^{-1} is seen. Similar to the case of XH$^{(n)}$, illumination with the HeNe laser results in the appearance of a new line at 2489 cm^{-1} at the expense of the main signal at 2471 cm^{-1}.

The frequency ratio of the photoinduced lines at 3358 and 2489 cm^{-1} is 1.35, which is close to the value expected for an harmonic oscillator that consists of a hydrogen atom bound to an oxygen atom, $\sqrt{\mu_D/\mu_H}=1.37$, where μ_H and μ_D are the reduced masses of the ^{16}O-H and ^{16}O-D units, respectively. Based on this we conclude that the 3358 cm^{-1} line is a local vibrational mode of the O-H species.

In order to investigate the relation between the photoinduced 3358 cm^{-1} line and the 3326 cm^{-1} line of the XH complex, IR absorption spectra at different stages of the subband gap illumination were obtained. The results are presented in Fig. 2. It shows the integrated intensity of the 3358 cm^{-1} mode as a function of the reduction in the intensity of the main signal at 3326 cm^{-1}. As follows from the

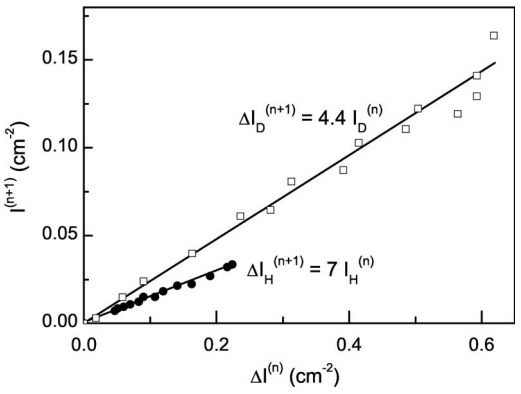

FIG. 2. Integrated absorption coefficients of photoinduced lines at 3358 and 2489 cm^{-1}, $I^{(n+1)}$, as a function of the reduction in the main signals at 3326 and 2471 cm^{-1}, $\Delta I^{(n)}$, respectively.

figure, the two signals are linearly related. The best fit of the experimental data shown by the solid lines reveals that the intensity of the photoinduced 3358 cm^{-1} mode is a factor of $\kappa_H=7\pm1$ weaker than the corresponding reduction in the $XH^{(n)}$ signal. This factor was found to be independent of the ZnO samples, which suggests that the 3326 and 3358 cm^{-1} lines are due to different charge states of the same defect. Similar behavior was found for the XD complex (see Fig. 2), although the value of $\kappa_D=4.4\pm0.7$ is somewhat less than that of XH.

At this stage we are uncertain about the charge states of the XH complex giving rise to the 3326 and 3358 cm^{-1} modes. Two possibilities can be considered: (i) photoinduced transition of an electron(s) from a defect level E_c-E_{XH} into the conduction band and (ii) photoinduced transition of an electron(s) from the valence band onto the defect level. Since all ZnO samples investigated in this work have *n*-type conductivity, the second possibility should be ruled out. Moreover, taking into account the fact that only two IR modes of the XH complex were detected, we suggest that the 3326 and 3358 cm^{-1} lines are local vibrational modes of $XH^{(n)}$ and $XH^{(n+1)}$, respectively.

The integrated absorption coefficient *A* of a local vibrational mode due to the O-H bond of the XH complex can be found from[30]

$$A=\int \alpha(\sigma)d\sigma=\frac{\pi e^{*2}N}{n_r c^2 \mu_{O\text{-}H}}. \quad (1)$$

Here, *N* is the concentration of the defect, e^* the effective charge, n_r is the refractive index, *c* the velocity of light, $\mu_{O\text{-}H}$ the reduced mass of the oscillator, and $\sigma=\lambda^{-1}$ the wave number.

It follows from Eq. (1) that the value of *A* quadratically depends on e^*. From here we find that the ratio of the effective charges of the O-H (O-D) bond $e_n^*/e_{n+1}^*=\sqrt{\kappa_{H(D)}}\approx2.6(2.1)$.

Such a behavior is not surprising since the microscopic structure of a point defect and hence the effective charge of a corresponding harmonic oscillator should depend on the charge state. A well-known example of this kind is bond-centered hydrogen, H_{BC}, in silicon.[31] The local vibrational mode of H_{BC}^+ gives rise to the 1998 cm^{-1} absorption line as measured at 10 K.[32,33] Band-gap light causes a fraction of H_{BC}^+ to convert into H_{BC}^0.[34] This conversion results in the decrease in the 1998 cm^{-1} line intensity without, however, noticeable appearance of an absorption line due to H_{BC}^0.[33] This behavior is explained by the considerably smaller value of e_0^* in the neutral-charge state of H_{BC} compared to that of e_+^*.[33] The similarity between H_{BC} and XH favors a negative value of *n*.

Since the ZnO samples employed in this study were *c*-cut wafers, defects consisting of O-H bonds aligned parallel to *c* cannot be detected by IR absorption at normal incidence of the light beam. To exclude the possibility that some amount of $XH^{(n+1)}$ escaped observation due to alignment parallel to the *c* axis, IR absorption measurements with polarized light for a sample turned at a 45° angle with respect to the $[10\bar{1}0]$ axis were also performed. No extra mode, which might appear because of the subband gap illumination, was detected. Moreover, the polarization properties of the 3326 and 3358 cm^{-1} lines were found to be identical. We take this as an indication that no O-H bond reorientation of the XH complex takes place at 10 K and thus all charge states of the defect are detected in our measurements.

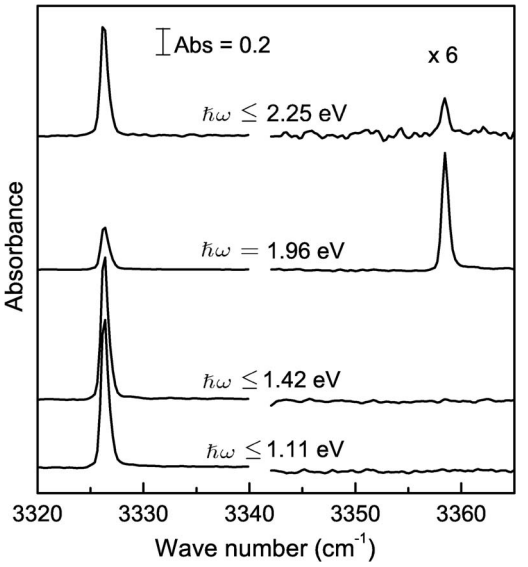

FIG. 3. IR absorption spectra obtained at 7 K for a ZnO sample treated in the H_2 gas at 725 °C after illumination by the quartz lamp through low-pass filters with the cut-off energies of 2.25, 1.42, and 1.12 eV. A spectrum measured after illumination from the HeNe laser ($\hbar\omega=1.96$ eV) is given for comparison. Illumination time (top to bottom) was 1, 1, 4, and 4 h.

B. Wavelength dependence of the $XH^{(n)}$ to $XH^{(n+1)}$ transition

In order to get insight into the position of the E_c-E_{XH} level in the band gap of ZnO, the wavelength dependence of the $XH^{(n)}$ to $XH^{(n+1)}$ conversion was investigated. The experiment was done as follows. First, a ZnO sample was cooled down in dark to approximately 10 K and an IR absorption spectrum was taken. Subsequently the sample was exposed to subband gap illumination from the built-in quartz light source of the FTIR spectrometer through a low-pass filter (see Sec. II). GaP, GaAs, and Si wafers were employed as low-pass filters. The cut-off frequencies of these filters determined by the corresponding band gaps are 2.25 eV, 1.42 eV, and 1.11 eV, respectively. After the illumination IR spectra were recorded. The results of this experiment are presented in Fig. 3.

As follows from the figure, the subband gap illumination of ZnO samples with energies below 1.96 eV does not result in the appearance of the $XH^{(n+1)}$ signal at 3358 cm^{-1}. The accuracy of this experiment does not allow us to determine the exact position of the E_{XH} level in the band gap of ZnO. A rough estimate gives $E_c-1.7\pm0.3$ eV. Such an energy strongly suggests that the XH defect has a deep level in the band gap and cannot be assigned to a shallow donor as previously suggested.[9]

C. Temperature dependence of $XH^{(n+1)}$ to $XH^{(n)}$ transition

The conversion from $XH^{(n)}$ to $XH^{(n+1)}$ is completely reversible at elevated temperatures. The conversion rate was

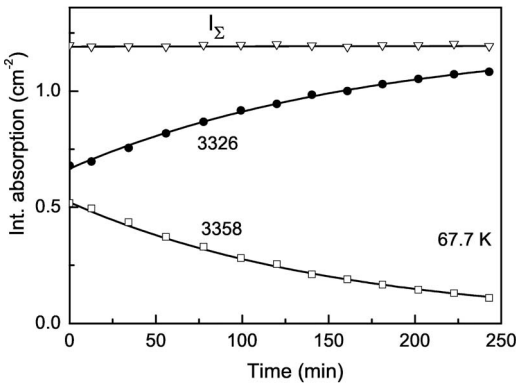

FIG. 4. Integrated absorption obtained for the 3326 (●) and 3358 cm^{-1} (□) lines at about 68 K. Solid lines are the best-fit curves.

investigated as a function of temperature. The experiment was done as follows. First, a ZnO sample was cooled down to about 7 K in the dark. Subsequently, it was illuminated with the HeNe laser until the 3358 cm^{-1} line appeared in the spectrum with an appreciable intensity. The sample was then annealed at the temperature of interest and IR spectra were measured as a function of time.

Figure 4 shows integrated intensities of the 3326 and 3358 cm^{-1} IR absorption lines obtained at about 68 K. Note that for presentation purposes the intensity of the 3358 cm^{-1} signal was multiplied by the proportionality factor of $\kappa_H=7$, which was determined in the previous subsection. Additionally, a weighted sum of the two signals, $I_\Sigma=I_{3326}+\kappa_H I_{3358}$, is given. As mentioned previously, I_Σ remains constant and is independent of the measurement time.

The solid lines in the figure are the best-fit curves obtained with the assumption that the back conversion from $XH^{(n+1)}$ to $XH^{(n)}$ can be described by a simple exponential decay. Here we assumed that $I_{3326} \propto a-\exp(-t/\tau)$ and $I_{3358} \propto \exp(-t/\tau)$, where a is a constant that depends on the initial conditions at $t=0$. From the data presented in the figure we find that $\tau=173$ min at 68 K.

The value of τ was determined at different temperatures for both the XD and XH complexes. The results are presented in Fig. 5. It follows from the figure, that within the

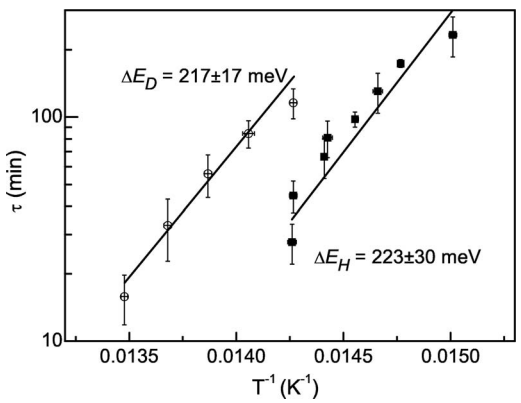

FIG. 5. Conversion time τ from $XH^{(n+1)}$ to $XH^{(n)}$ as a function of temperature obtained for the XH (■) and XD (○) complexes.

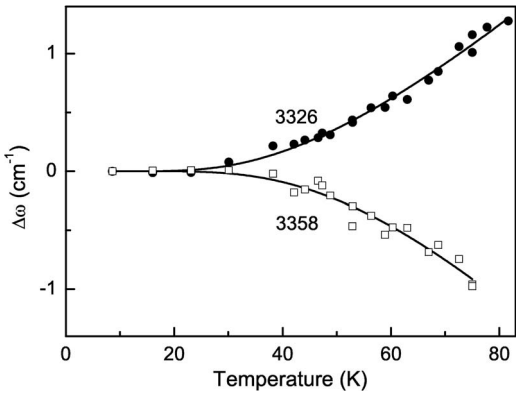

FIG. 6. Temperature dependence of the LVM frequencies due to the $XH^{(n)}$ (●) and $XH^{(n+1)}$ (□) complexes. The frequencies are given with respect to the values obtained at 7 K. Solid lines are the best-fit curves (see text).

error bars of our experiment, the back conversion from $XH^{(n+1)}$ to $XH^{(n)}$ is thermally activated with a conversion rate that can be approximated by $\tau^{-1}=\tau_0^{-1}\exp(\Delta E/kT)$. From the best-fit values shown in Fig. 5 by the solid lines we find that the activation energy $\Delta E=220\pm30$ meV is basically independent of the hydrogen isotope. Contrary to that, the value of τ_0 was found to be approximately 3.4×10^{-15} s and 3.2×10^{-14} s for XH and XD, respectively. That is, the back conversion from $XH^{(n+1)}$ to $XH^{(n)}$ is slower if hydrogen is replaced by deuterium. We believe, however, that the difference in τ_0 between the hydrogen isotopes is not caused by the nature of the XH complex.

D. Temperature dependence of the LVM frequencies

Figure 6 shows the temperature dependence of the LVM frequencies due to the $XH^{(n)}$ and $XH^{(n+1)}$ complexes. Note that the LVM temperature dependence of the $XH^{(n)}$ defect has been investigated previously.[35] The behavior of the LVM frequency changes as the charge state of the XH defect changes: the mode of $XH^{(n)}$ (3326 cm^{-1} line) experiences a "blueshift" with temperature whereas the frequency of the $XH^{(n+1)}$ (3358 cm^{-1} line) complex decreases as the temperature increases.

To fit the data that are presented in Fig. 6 we employ a model proposed by Persson and Ryberg which takes into account a coupling of the O-H harmonic vibration anharmonically with an exchange mode E_0 through a parameter $\delta\omega$.[36] In the framework of this model, the following expression is obtained for the frequency shift $\Delta\omega$ of the LVM:

$$\Delta\omega = \frac{\delta\omega}{\exp(E_0/kT)-1}. \tag{2}$$

The best-fit parameters for Eq. (2) were found to be $E_0=16.3$ meV, $\delta\omega=-10.6$ cm^{-1}, and $E_0=12.8$ meV and $\delta\omega=6.8$ cm^{-1} for $XH^{(n+1)}$ and $XH^{(n)}$, respectively. The corresponding fitting curves are presented in Fig. 6 by the solid lines and are in a reasonable agreement with the experimental data.

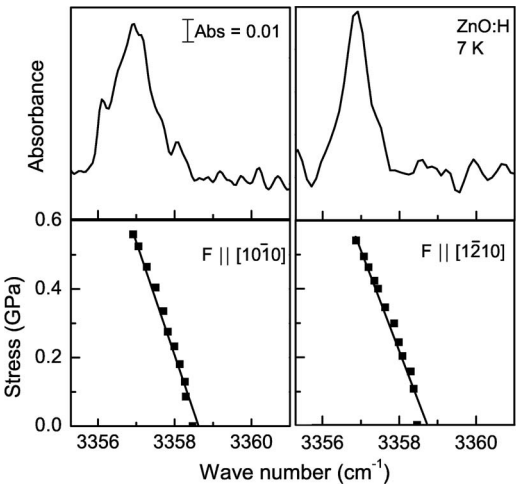

FIG. 7. IR absorption spectra and shift patterns obtained at 7 K for the 3358 cm^{-1} line under uniaxial stress applied parallel to [10$\bar{1}$0] and [1$\bar{2}$10].

E. Uniaxial stress measurements

Further insight into the microscopic properties of the XH complex can be obtained from uniaxial stress experiments. Uniaxial stress studies of the 3326 cm^{-1} vibrational mode due to XH$^{(n)}$ were reported in Ref. 29. It was found that the line does not split for stress applied along the c axis and splits into two components for $F\|[10\bar{1}0]$ and [1$\bar{2}$10], which favors a monoclinic symmetry of the XH$^{(n)}$ complex.[37]

Figure 7 shows the behavior of the 3358 cm^{-1} line of the XH$^{(n+1)}$ complex under uniaxial stress applied parallel to [10$\bar{1}$0] and [1$\bar{2}$10]. As one can see, the 3358 cm^{-1} line shifts with the stress at rate of -3.0 ± 0.5 and -3.2 ± 0.6 cm^{-1}/GPa for $F\|[10\bar{1}0]$ and [1$\bar{2}$10], respectively. We note that for the purposes of the uniaxial stress measurements an appreciable intensity of the 3358 cm^{-1} line was detected only in the c-cut wafers provided by Cermet (see Sec. II). For such a geometry, however, measurements with the stress applied parallel to the c axis were not possible, which explains the missing data for $F\|c$.

In the linear approximation, the frequency of a nondegenerate LVM shifts with the stress σ_{ik} as

$$\Delta\omega = \sum_{i,k} A_{ik}\sigma_{ik}, \tag{3}$$

where A_{ik} are the components of the piezospectroscopic tensor. The stress lifts the orientational degeneracy that results in a splitting of the LVM. The number and intensity of the stress-induced components depend on the defect symmetry, stress direction, and measurement geometry. A general consideration of the splitting patterns of point defect energy levels in wurtzite crystals was given by McGlynn and Henry.[37]

As pointed out already, the 3326 cm^{-1} line splits into one, two, and two components for the stress directions parallel to c, [10$\bar{1}$0], and [1$\bar{2}$10], respectively, which implies that the symmetry of the XH$^{(n)}$ complex is monoclinic. Interestingly, the 3358 cm^{-1} line of the XH$^{(n+1)}$ complex does not split, which seems to suggests that the symmetry of the defect is trigonal. This would imply that the O-H bond of the XH$^{(n+1)}$ complex is aligned parallel to the c axis and hence should not be visible in the IR spectra obtained at normal incidence of the light beam of our c-cut wafers. This obvious contradiction with the experimental data leads us to the conclusion that the point group of the XH defect remains monoclinic in the $n+1$ charge state with the OH bond of the XH defect oriented perpendicular to the c axis. The missing splitting of the 3358 cm^{-1} line we explain by the modified values of A_{ij} so that $A_{xx}\approx A_{yy}$. We believe that it is a substantial full width at half maximum of the IR lines that masks the splitting of the LVM under uniaxial stress.

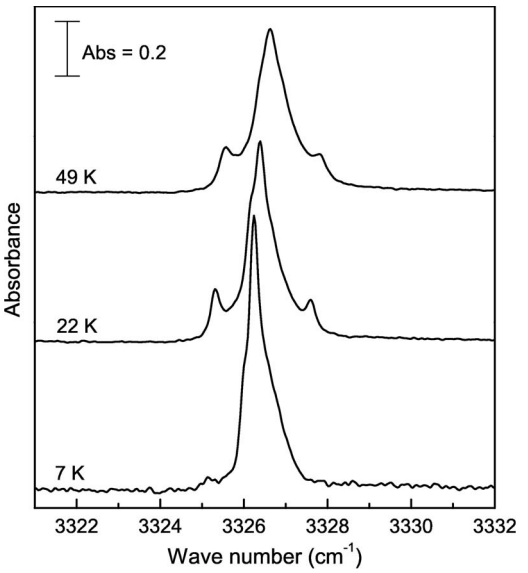

FIG. 8. IR absorption spectra of the 3326 cm^{-1} line recorded with a resolution of 0.05 cm^{-1} at 7, 22, and 49 K.

F. Fine structure of the 3326 cm^{-1} line

IR absorption spectra of the 3326 cm^{-1} line recorded at 7, 22, and 49 K with a resolution of 0.05 cm^{-1} are shown in Fig. 8. As the temperature increases two satellites, shifted by -1.1 and 1.2 cm^{-1} from the main line, appear in the spectra. The relative positions of these peaks with respect to the 3326 cm^{-1} line are independent of the temperature. The IR absorption lines experience temperature broadening, and at $T>70$ K the side peaks can no longer be resolved.

In addition to the temperature-induced satellites, the main signal at 3326 cm^{-1} also reveals a fine structure, which seems to be independent of the temperature. It manifests itself in at least one poorly resolved shoulder "redshifted" by approximately 0.25 cm^{-1} from the maximum of the 3326 cm^{-1} line. A possible origin for this fine structure could be an isotope shift due to an unidentified impurity X comprising the XH complex (see, for example, Ref. 19).

Asymmetry of the XH$^{(n)}$ signal is another feature revealed in the IR spectra taken with high resolution. Within the error bars of our experimental setup, this asymmetry correlates with the concentration of shallow donors due to H_{BC} (see next subsection). This strongly suggests a Fano resonance[38] between the local vibrational mode and the continuum of the

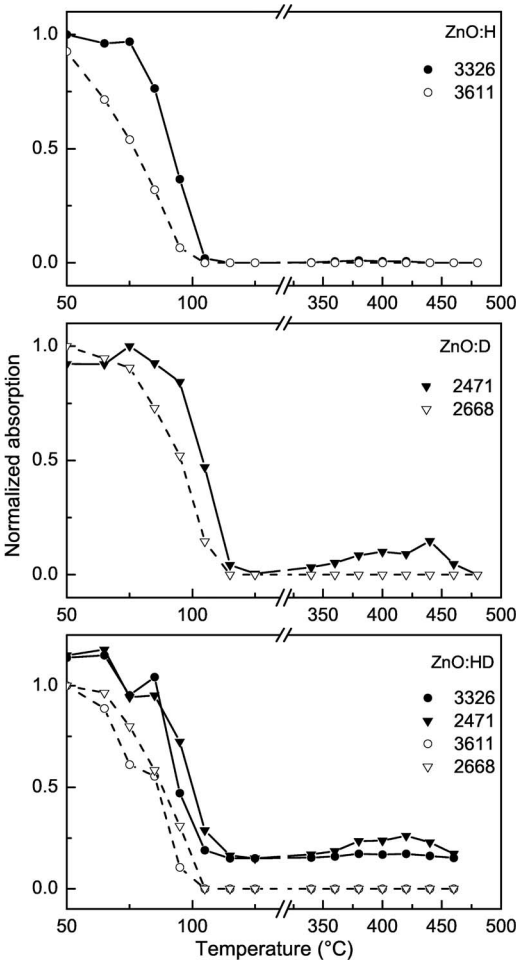

FIG. 9. Normalized integrated intensities of the LVMs due to H_{BC} (○), $XH^{(n)}$ (●), D_{BC} (▽), and $XD^{(n)}$ (▼) as a function of the annealing temperature. The samples were hydrogenated in the H_2 (top), D_2 (mid), and a mixture of H_2+D_2 (bottom) gases at 725 °C. For the sake of convenience, the data for $XH^{(n)}$ and $XD^{(n)}$ in the bottom panel are offset by 0.15.

electronic states in the conduction band as an explanation for the line shape of the 3326 cm^{-1} mode. A similar situation was recently reported for the E_1(LO) phonon mode in ZnO coupled with electronic transitions of H_{BC}.[12] The fine structure of the 3326 cm^{-1} signal, however, did not allow us to investigate this issue quantitatively.

G. Thermal stability of XH

Figure 9 shows integrated intensities of the LVMs due to $XH^{(n)}$ (3326 cm^{-1}) and $XD^{(n)}$ (2471 cm^{-1}) as a function of annealing temperature. As mentioned already, our ZnO samples were *c*-cut wafers. This implies that local modes of O-H species aligned parallel to the *c* axis cannot be detected at normal incidence of the light beam. In order to bypass this problem the annealing series shown in the figure were obtained for a sample orientation turned at 45° angle with respect to the optical axis of the spectrometer.[24] Such a geometry allowed us to monitor the thermal stability of the local modes due to H_{BC} (3611 cm^{-1}) and D_{BC} (2668 cm^{-1}) also presented in the sample. What is important, no other hydrogen-related vibrational modes were detected in the course of these annealing experiments.

The stability of H_{BC} is determined by a thermally activated diffusion process with subsequent trapping by other impurities and/or the formation of interstitial H_2.[12,14] Provided hydrogen is the dominant impurity in ZnO, the hydrogen molecule becomes a main sink for H_{BC}. As a shallow donor, bond-centered hydrogen is ionized and positively charged at RT. The Coulomb repulsion between two H_{BC}^+ slows down the formation of H_2 and results in an apparent stability of H_{BC} up to 170 °C.[12]

It follows from the top panel of Fig. 9 that in Cermet ZnO both the H_{BC} and XH complexes anneal out simultaneously at about 105 °C (see also Ref. 24), which indicates that for such a material the reaction

$$H_{BC}^+ + H_{BC}^+ \rightleftharpoons H_2 \tag{4}$$

is not the only process that governs thermal stability of H_{BC}.

Upon substitution of hydrogen with deuterium (mid panel) the annealing temperature increases by approximately 10 °C. Similar behavior was documented for a number of hydrogen-related complexes in ZnO and is normally explained by the difference in the zero-point energies of the O-H and O-D species.[12,17,39]

The different annealing temperatures of XH and XD are, however, a new result. To get insight into the nature of XH, an annealing series for a ZnO sample treated in a mixture of H_2 and D_2 was also performed. The results are presented in the bottom panel of the figure. Under these conditions XD remains more stable than XH although the annealing temperature is reduced by approximately 10 °C compared to the sample treated in D_2 gas.

We speculate that the experimental data presented in Fig. 9 are consistent with the reaction

$$H_{BC}^+ + XH^{(n)} \rightleftharpoons X + H_2. \tag{5}$$

The following findings can be understood in the framework of this model. (i) H_2 is invisible in IR absorption and because of this has long been considered as "hidden" hydrogen in ZnO.[12,40] Having the hydrogen molecule as the product of the reaction given by Eq. (5) explains why no other IR absorption signals are detected when H_{BC} and XH are gone. (ii) Interaction between H_{BC} and XH accounts for the similar annealing behavior of the two defects (see also Ref. 24). (iii) The relative stability of XD compared to XH follows from the higher diffusivity of H_{BC} with respect to D_{BC} resulting from different zero-point energies of hydrogen isotopes.[12] (iv) Formation of the HD molecule explains why XD anneals out earlier in the sample treated in the H_2 and D_2 mixture compared to that of pure D_2 gas. (v) As mentioned already the Coulomb repulsion between two H_{BC}^+ accounts for the apparent stability of the bond-centered hydrogen up to 170 °C.[12] On the other hand, the charge state of $XH^{(n)}$ is expected to be either neutral or negative. The missing Coulomb barrier between H_{BC}^+ and $XH^{(n)}$ speeds up the formation of H_2 and results in the reduction in the annealing temperature of the bond-centered hydrogen down to 105 °C. (vi) According to first-principles calculations, H_{BC} is the ground

state of hydrogen in ZnO for nearly all Fermi level energies except those close to the conduction band minimum.[3] Bond-centered hydrogen is a shallow donor with an ionization energy of 53 meV.[12] The concentration of H_{BC} immediately after thermal treatment in H_2 gas as determined by the integrated intensity of the 3611 cm^{-1} line is 2×10^{17} cm^{-2}.[12] This amount ensures that the Fermi level is positioned at the bottom of the conduction band and hence H_{BC} is not stable against the formation of H_2.[14] Further annealing at around 450 °C, however, shifts the Fermi level deeper into the band gap thus making the formation of H_{BC} energetically favorable again. This manifests itself in the reappearance of H_{BC} and XH (see Fig. 9 and Ref. 24). Finally, at temperatures above 500 °C hydrogen diffuses out so that no other hydrogen-related defects are left in the sample.

IV. DISCUSSION

First we comment on previous studies of light-induced effects of the XH complex. Vapor phase grown, Cermet, and Eagle Picher ZnO samples were investigated by Shi *et al.*[24] The authors found that illumination of Cermet and Eagle Picher ZnO with a broad band tungsten lamp results in the reduction in the intensity of the 3326 cm^{-1} line. Nickel employed a 450 nm LED as a secondary light source and also found that the intensity of the 3326 cm^{-1} line was reduced with the illumination time.[28] No signal which would appear in the IR spectra at the expense of the 3326 cm^{-1} line was detected. Presumably Shi *et al.* and Nickel did not detect the 3358 cm^{-1} line because of its weak intensity.

Nickel also studied a "recovery rate" of the 3326 cm^{-1} line subjected to subband gap illumination.[28] It was found that the intensity of this signal does not recover for temperatures below 30 K. With increasing temperature the recovery rate raises and reaches a local maximum at about 45 K. After that it decreases and comes to a minimum at about 70 K. Further on, the recovery rate monotonously enhances with temperature.

These results contradict our experimental findings, which clearly indicate a typical Arrhenius behavior with an activation energy of around 220 meV (see Fig. 5). We speculate that the complex dependence of the recovery rate reported by Nickel results from a short annealing time of 5 min.

Three models have been proposed for the XH complex in the literature so far. These are isolated hydrogen at the antibonding lattice site (H_{AB}),[9] a complex of calcium-hydrogen,[25] and a Zn vacancy passivated with a single hydrogen atom, ($V_{Zn}H$).[27] Below we discuss these models.

H_{AB}. The 3326 cm^{-1} line was first observed by McCluskey *et al.* in Cermet ZnO and was tentatively assigned to the H_{AB} complex where the O-H bond forms an angle of 110° with the *c* axis.[9] Calculated vibrational frequencies of H_{AB} are in agreement with the experimental value.[3,26,41,42] Further indication that hydrogen at the antibonding site of the ZnO lattice might be responsible for the XH complex came from experiments on hydrostatic compression. It was established that the 3326 cm^{-1} line shifts with the rate of -1.5 ± 0.3 cm^{-1}/GPa,[23,29] which is in qualitative agreement with the theoretical prediction of -4 cm^{-1}/GPa.[42,43]

The H_{AB} model of the 3326 cm^{-1} line, however, meets serious difficulties. First of all, theory finds that the formation energy of H_{AB} is 0.15–0.3 eV higher than that of H_{BC}, which implies that hydrogen at the antibonding site cannot occur in high concentrations at low temperatures.[26,41,42,44] No explanation was also given for why the intensity of the 3326 cm^{-1} line depends on the ZnO sample. The activation energy of hydrogen motion in the XH complex was determined to be above 0.7 eV,[27] which contradicts the microscopic model of H_{AB} and the results of first-principles calculations predicting a reorientation barrier of around 0.2 eV.[45,46] Finally, theory finds that H_{AB} is a shallow donor in ZnO.[3] Our study, however, reveals that the XH complex has a deep level in the band gap.

Based on this, we conclude that it is very unlikely that H_{AB} is the defect giving rise to the 3326 cm^{-1} line.

CaH. Secondary-ion mass spectrometry and delayed gamma neutron activation analysis of Cermet ZnO revealed that this material contains approximately 4×10^{16} cm^{-3} of Ca atoms. On the other hand, the Ca content in Eagle Picher ZnO was found to be below the detection limit of these techniques. Since the intensity of the 3326 cm^{-1} line is the strongest in the Cermet material, it was suggested that Ca is the missing constituent of the XH complex.[25]

First-principles theory finds that complex of substitutional Ca at the Zn site with hydrogen bound to the O atom at the antibonding site with the O-H bond aligned "perpendicular" to the *c* axis could partially account for the experimental data.[26,44] In particular, the LVM frequency was found to be consistent with the experimental value of 3326 cm^{-1}. On the other hand, for complexes of hydrogen with Ca, Sr, and Na, where hydrogen is positioned at the AB site, the calculated LVM frequencies are similar within 30 cm^{-1}, thus making impurity identification based solely on the LVM frequency basically impossible.[44]

More importantly, theory finds that the binding energy of hydrogen in the CaH complex is around 0.5 eV.[26,44] Such a value is consistent with the low thermal stability of the 3326 cm^{-1} line. We note that annealing mechanism of the H_{BC} and XH complexes given by Eq. (5) does not contradict the theoretical dissociation energy of CaH.

The CaH model has, however, a serious drawback. Electrical activity of CaH has not been considered theoretically so far. In the first approximation, however, we might assume that it is similar to that of isolated H_{AB}. If so, CaH is expected to act as a shallow donor, which is not consistent with the influence of subband gap light on the intensity of the 3326 cm^{-1} line. The similarity between CaH and isolated H_{AB}, however, comes from the isovalent character of Ca in ZnO and has to be verified by first-principles calculations. Therefore, we do not rule out the CaH model of the XH complex but further theoretical studies are called for.

$V_{Zn}H$. The Zn vacancy is a double acceptor in ZnO and as such always occurs in the negative-charge state in *n*-type material. The high mobility of isolated hydrogen and the Coulomb attraction between H_{BC}^{+} and V_{Zn}^{2-} could easily result in the formation of complexes $V_{Zn}H_n$. Indeed, it was shown that $V_{Zn}H_2$ gives rise to absorption lines at 3312 and 3350 cm^{-1}.[13] Contrary to that, no unambiguous identifica-

TABLE I. Comparison between experimental and theoretical frequencies of $V_{Zn}H_n$ in ZnO (cm^{-1}). The factor of $k=3312/3228$ was used to obtain the scaled values (to account for the difference between calculated and experimental values for O-H$\|c$ in $V_{Zn}H_2$).

Structure		Expt.[a]	Theory[b]	
			As calculated	Scaled ($\times k$)
$V_{Zn}H_2$	O-H$\|c$	3312	3228	3312
	O-H$\perp c$	3350	3267	3352
$V_{Zn}H^0$	O-H$\perp c$		3272	3357
$V_{Zn}H^0$	O-H$\|c$		3255	3340

[a]Reference 13.
[b]Reference 41.

tion of the $V_{Zn}H$ complex has been reported so far.

Experiments on stress-induced dichroism of hydrogen LVMs in ZnO revealed that activation energies of hydrogen motion in $V_{Zn}H_2$ and that of the XH complex exceed 0.7 eV.[27] This finding suggested the negative-charge state of $V_{Zn}H$ as a model for the 3326 cm^{-1} line.

Vibrational frequencies and formation energies of several $V_{Zn}H_n$ complexes were investigated theoretically by a number of groups.[26,41,44] There is a general consensus that hydrogen occupies an "internal" volume of the Zn vacancy. Two hydrogen atoms result in complete passivation of V_{Zn} and formation of $V_{Zn}H_2$. Wardle *et al.* find that the two O-H bonds comprising the defect are aligned parallel and perpendicular to the *c* axis.[41] The corresponding local modes at 3228 and 3267 cm^{-1} are in reasonably good agreement with the experimental data.

The microscopic structure of $V_{Zn}H$ depends on the charge state of the defect. Bang *et al.* found that the O-H bond comprising $V_{Zn}H^0$ is aligned parallel to the *c* axis whereas in $V_{Zn}H^-$ it prefers to be oriented perpendicular to *c*.[44] The difference in energy between different orientations of the O-H bond in each charge state is rather marginal (within 20 meV).[41,46] Even though, theory seems to favor $V_{Zn}H^-$ as a model for the 3326 cm^{-1} line.

The comparison between theoretical and experimental LVM frequencies of $V_{Zn}H$ is difficult since most authors discuss only the neutral-charge state of the defect in its energetically most favorable configuration. For this reason, we consider only $V_{Zn}H$ in the neutral-charge state with the O-H bond aligned perpendicular to the *c* axis. To facilitate comparison with experiment, known LVM frequencies of $V_{Zn}H_2$ should be employed as a benchmark. The results of such a comparison are presented in Table I. Note that the LVM frequency of O-H$\|c$ in $V_{Zn}H_2$ was used to obtain a scaling factor $1.026=3312/3228$. It follows from the table that after correction for systematic error, the LVM frequency of $V_{Zn}H^0$ equals 3357 cm^{-1}, which is in remarkable agreement with the 3358 cm^{-1} mode of $XH^{(n+1)}$. Thus, local mode analysis also favors the $V_{Zn}H$ model for the XH defect.

First-principles calculations by Wardle *et al.*[41] reveal that $V_{Zn}H$ is a deep acceptor giving rise to a $(-/0)$ level in the band gap positioned at $E_v+0.46$ eV. This is only in qualitative agreement with our estimate of the energy level of the XH defect at $E_c-1.7\pm0.3$ eV. Note, however, that the subband gap illumination provides only a rough estimate for the energy level in the band gap. The error bars cited reflect only the difference in energy of the light quanta resulted in the appearance of the 3358 cm^{-1} line.

EPR studies of electron-irradiated Eagle Picher ZnO were performed by Evans *et al.*[47] These authors reported an EPR signal, which was identified as $V_{Zn}H$ in the neutral-charge state. The transition $V_{Zn}H^-\rightarrow V_{Zn}H^0$ was achieved via subband gap illumination with a threshold energy at about 2.5 eV. Based on this, the authors suggested that the $(-/0)$ level of $V_{Zn}H$ is positioned at roughly $E_v+0.9$ eV, which is somewhere in between the theoretical prediction and the value determined in this study.

The temperature dependences of the LVM frequencies presented in Fig. 6 can be also understood in the framework of the $V_{Zn}H$ model. Normally, the LVM frequency of a defect increases with decreasing temperature resulting from strengthened bonds arising from the lattice contraction. In contrast, the LVM frequency of the $XH^{(n)}$ defect shifts upwards with temperature. The same behavior was documented for the LVMs of $V_{Zn}H_2$ and was tentatively explained by the buckling of the hydrogen atom from the regular bond direction.[13,48] The off-axis orientation of the O-H bonds in the $V_{Zn}H_2$ complex comes from repulsive forces pushing away the two hydrogen atoms sharing the internal volume of the Zn vacancy. In the case of $V_{Zn}H^-$, an electron occupying O orbital would also result in the reduction in the volume inside the Zn vacancy and displacement of the O-H bond.

An off-axis orientation of the O-H bond also implies that apart from the global minimum, additional minima may exist, which could result in somewhat different LVM frequencies than those of the ground state. When the temperature rises, the higher states become occupied giving rise to side peaks at the main line. This situation was observed for the LVMs of $V_{Zn}H_2$.[13] The results presented in Fig. 8 are also consistent with an off-axis orientation of the O-H bond in the $XH^{(n)}$ complex.

On the other hand, $V_{Zn}H^0$ should provide more room for hydrogen in the internal volume of the Zn vacancy. This results in the regular orientation of the O-H bond and a typical temperature behavior of the 3358 cm^{-1} mode of the $XH^{(n+1)}$ complex (see Fig. 6).

The $V_{Zn}H$ model of the XH defect suggests an alternative to the annealing scheme given by Eq. (5). The disappearance of the 3326 cm^{-1} line from the spectra as the H_{BC} signal fades away is then a function of the Fermi level, which is tied to the concentration of the bond-centered hydrogen. As the Fermi level moves deeper into the band gap, a part of $V_{Zn}H^-$ converts into $V_{Zn}H^0$, which according to theory[41,44] should result in a flip of the O-H bond to the orientation parallel to the *c* axis. Note that the corresponding LVM frequency is expected to be at 3340 cm^{-1} (see Table I).

Since all ZnO samples where the 3326 cm^{-1} line occurs with a reasonable intensity are *c*-cut wafers, this implies that $V_{Zn}H^0$ cannot be detected in IR absorption at normal incidence of the light beam. Moreover, the difference in effective charges between the 3326 and 3358 cm^{-1} lines (see Sec. III A) strongly indicates that the expected intensity of the local mode due to $V_{Zn}H^0$ could be weak.

The $V_{Zn}H$ model of the XH defect also suggests that at some stage of the annealing series the formation of $V_{Zn}H_2$ might be expected to take place. IR absorption studies performed by Shi *et al.*[40] revealed that after an anneal at 400 °C, the local mode of $V_{Zn}H_2$ at 3350 cm^{-1} (O-H $\perp c$) did appear in the IR spectrum (see Fig. 2 in Ref. 40).

Our annealing experiments, which results are presented in Fig. 9, were performed for the sample orientation turned at 45° with respect to the optical axis of the spectrometer. However, neither $V_{Zn}H_2$ nor any other lines were detected in the course of the annealing series. Although the failure to detect an LVM due to $V_{Zn}H^0$ might well result from the weak intensity of this signal, this casts some doubts on the $V_{Zn}H$ model of the 3326 cm^{-1} line.

Summarizing this section, we conclude that only the H_{AB} model of the XH complex can be ruled out with certainty. Contrary to isolated hydrogen at the antibonding site, CaH and $V_{Zn}H$ can explain the majority (but not all) of the experimental data. The drawbacks of both models, however, prevent us from a definite choice. An involvement of another constituent in the formation of XH cannot be completely excluded either.

V. CONCLUSIONS

The results of an IR absorption study of a hydrogen defect in ZnO that results in a local vibrational mode at 3326 cm^{-1} are presented. We show that subband gap illumination results in the appearance of a new IR absorption line at 3358 cm^{-1} at the expense of the main signal at 3326 cm^{-1}. Based on the anticorrelation between the two lines as well as the results of isotope substitution experiments, it is concluded that both signals are due to stretch modes of an O-H bond associated with the same defect in different charge states. The energy quanta of the subband gap light strongly suggest that this defect has a deep level in the band gap of ZnO at roughly $E_c - 1.7$ eV. This rules out isolated hydrogen at the antibonding site which was an early model for the 3326 cm^{-1} line. Additionally, the results on thermal stability, uniaxial stress response, and the temperature dependence of the transition rates between the two charge states of this defect are presented. It is shown that the CaH and $V_{Zn}H$ models for the 3326 cm^{-1} line also cannot satisfactorily explain all experimental data.

ACKNOWLEDGMENTS

This work was supported by the European Regional Development Fund and the Free State of Saxony. Work by M.S. was supported by NSF under Grant No. DMR 0802278 and by the Humboldt Foundation.

*frank.herklotz@physik.tu-dresden.de

[1] E. Mollwo, Z. Phys. **138**, 478 (1954).
[2] D. G. Thomas and J. J. Lander, J. Chem. Phys. **25**, 1136 (1956).
[3] C. G. Van de Walle, Phys. Rev. Lett. **85**, 1012 (2000).
[4] A. Janotti and C. G. Van de Walle, Nature Mater. **6**, 44 (2007).
[5] S. F. J. Cox *et al.*, Phys. Rev. Lett. **86**, 2601 (2001).
[6] K. Shimomura, K. Nishiyama, and R. Kadono, Phys. Rev. Lett. **89**, 255505 (2002).
[7] D. M. Hofmann, A. Hofstaetter, F. Leiter, H. J. Zhou, F. Henecker, B. K. Meyer, S. B. Orlinskii, J. Schmidt, and P. G. Baranov, Phys. Rev. Lett. **88**, 045504 (2002).
[8] B. K. Meyer *et al.*, Phys. Status Solidi B **241**, 231 (2004).
[9] M. D. McCluskey, S. J. Jokela, K. K. Zhuravlev, P. J. Simpson, and K. G. Lynn, Appl. Phys. Lett. **81**, 3807 (2002).
[10] C. H. Seager and S. M. Myers, J. Appl. Phys. **94**, 2888 (2003).
[11] E. V. Lavrov, F. Börrnert, and J. Weber, Phys. Rev. B **72**, 085212 (2005).
[12] E. V. Lavrov, F. Herklotz, and J. Weber, Phys. Rev. B **79**, 165210 (2009).
[13] E. V. Lavrov, J. Weber, F. Börrnert, C. G. Van de Walle, and R. Helbig, Phys. Rev. B **66**, 165205 (2002).
[14] E. V. Lavrov, F. Herklotz, and J. Weber, Phys. Rev. Lett. **102**, 185502 (2009).
[15] A. Schildknecht, R. Sauer, and K. Thonke, Physica B **340-342**, 205 (2003).
[16] E. V. Lavrov and J. Weber, Phys. Status Solidi B **243**, 2657 (2006).
[17] E. V. Lavrov, J. Weber, and F. Börrnert, Phys. Rev. B **77**, 155209 (2008).
[18] E. V. Lavrov, F. Börrnert, and J. Weber, Phys. Rev. B **71**, 035205 (2005).
[19] G. A. Shi, M. Stavola, and W. B. Fowler, Phys. Rev. B **73**, 081201(R) (2006).
[20] S. J. Jokela and M. D. McCluskey, Phys. Rev. B **76**, 193201 (2007).
[21] F. G. Gärtner and E. Mollwo, Phys. Status Solidi B **89**, 381 (1978).
[22] S. J. Jokela, M. D. McCluskey, and K. G. Lynn, Physica B **340-342**, 221 (2003).
[23] S. J. Jokela and M. D. McCluskey, Phys. Rev. B **72**, 113201 (2005).
[24] G. A. Shi, M. Stavola, S. J. Pearton, M. Thieme, E. V. Lavrov, and J. Weber, Phys. Rev. B **72**, 195211 (2005).
[25] M. D. McCluskey and S. J. Jokela, Physica B **401-402**, 355 (2007).
[26] X.-B. Li, S. Limpijumnong, W. Q. Tian, H. B. Sun, and S. B. Zhang, Phys. Rev. B **78**, 113203 (2008).
[27] E. V. Lavrov, B. Börrnert, and J. Weber, Physica B **401-402**, 366 (2007).
[28] N. H. Nickel, Phys. Status Solidi B **243**, R51 (2006).
[29] E. V. Lavrov and J. Weber, Phys. Rev. B **73**, 035208 (2006).
[30] E. B. Wilson, J. C. Decius, and P. C. Cross, *Molecular Vibrations* (Dover, New York, 1980).
[31] V. A. Gordeev, R. F. Konopleva, V. G. Firsov, Y. V. Obukhov, Y. V. Gorelkinskii, and N. N. Nevinnyi, Hyperfine Interact. **60**, 717 (1990).
[32] H. J. Stein, Phys. Rev. Lett. **43**, 1030 (1979).
[33] M. Budde, Ph.D. thesis, University of Aarhus, 1998.

[34] B. B. Nielsen, K. B. Nielsen, and J. R. Byberg, in *Defects in Semiconductors 17*, edited by H. Heinrich and W. Jantsch (Trans Tech, Aedermannsford, Switzerland, 1994), Vols. 143-147, p. 909.
[35] M. D. McCluskey, S. J. Jokela, and W. M. H. Oo, Physica B **376-377**, 690 (2006).
[36] B. N. J. Persson and R. Ryberg, Phys. Rev. B **32**, 3586 (1985).
[37] E. McGlynn and M. O. Henry, Phys. Rev. B **76**, 184109 (2007).
[38] U. Fano, Phys. Rev. **124**, 1866 (1961).
[39] F. Börrnert, E. V. Lavrov, and J. Weber, Phys. Rev. B **75**, 205202 (2007).
[40] G. A. Shi, M. Saboktakin, M. Stavola, and S. J. Pearton, Appl. Phys. Lett. **85**, 5601 (2004).
[41] M. G. Wardle, J. P. Goss, and P. R. Briddon, Phys. Rev. B **72**, 155108 (2005).
[42] S. Limpijumnong and S. B. Zhang, Appl. Phys. Lett. **86**, 151910 (2005).
[43] M. G. Wardle, J. P. Goss, and P. R. Briddon, Appl. Phys. Lett. **88**, 261906 (2006).
[44] J. Bang, E. Choi, and K. J. Chang, J. Appl. Phys. **106**, 053522 (2009).
[45] M. G. Wardle, J. P. Goss, and P. R. Briddon, Phys. Rev. Lett. **96**, 205504 (2006).
[46] J. Bang and K. J. Chang, J. Korean Phys. Soc. **55**, 98 (2009).
[47] S. M. Evans, N. C. Giles, L. E. Halliburton, and L. A. Kappers, J. Appl. Phys. **103**, 043710 (2008).
[48] J. Coutinho, R. Jones, P. R. Briddon, and S. Öberg, Phys. Rev. B **62**, 10824 (2000).